Article:
Chen, C.-C., Huang, Y.-C., Ortega, A. et al. (2026) Sleep facilitates pattern separation through SK channel-mediated sparse coding. Current Biology, 36 (7). 1633-1643.e6. ISSN: 0960-9822

https://doi.org/10.1016/j.cub.2026.02.028

Article

Current Biology

Sleep facilitates pattern separation through SK channel-mediated sparse coding

Highlights

- Sleep deprivation selectively impairs pattern separation in *Drosophila*
- Sleep maintains sparse and decorrelated odor coding in the fly mushroom body
- Sleep loss enhances SK channel-mediated AHP in inhibitory APL neurons
- APL-specific SK knockdown rescues pattern separation after sleep deprivation

Authors

Chien-Chun Chen, Yu-Chun Huang, Antonio Ortega, ..., Yifan Wu, Andrew C. Lin, Sha Liu (刘沙)

Correspondence

sha.liu@kuleuven.be

In brief

Chen et al. report that sleep deprivation impairs pattern separation in *Drosophila* by disrupting sparse coding in the mushroom body. This deficit stems from enhanced SK channel-mediated afterhyperpolarization in inhibitory APL neurons. Knockdown of SK channels in APL neurons rescues the ability to discriminate similar odors after sleep loss.

Chen et al., 2026, Current Biology *36*, 1–11
April 6, 2026
https://doi.org/10.1016/j.cub.2026.02.028

CellPress

Current Biology

CellPress
OPEN ACCESS

Article

Sleep facilitates pattern separation through SK channel-mediated sparse coding

Chien-Chun Chen,[1,2,3] Yu-Chun Huang,[1,2,3] Antonio Ortega,[1,2,3] Raquel Suárez-Grimalt,[4,5,7] Erik Tedre,[1,3] El-Sayed Baz,[1,3,6] Yifan Wu,[1,2,3] Andrew C. Lin,[4,5] and Sha Liu (刘沙)[1,2,3,8,*]

[1]VIB-KU Leuven, Center for Neuroscience, Leuven 3000, Belgium
[2]KU Leuven, Department of Neurosciences, Leuven 3000, Belgium
[3]KU Leuven, Leuven Brain Institute, Leuven 3000, Belgium
[4]University of Sheffield, School of Biosciences, Sheffield S10 2TN, UK
[5]University of Sheffield, Neuroscience Institute, Sheffield S10 2TN, UK
[6]Suez Canal University, Zoology Department, Ismailia 41522, Egypt
[7]Present address: Freie Universität Berlin, Institute of Biology, 14195 Berlin, Germany
[8]Lead contact
*Correspondence: sha.liu@kuleuven.be
https://doi.org/10.1016/j.cub.2026.02.028

SUMMARY

The roles of sleep in priming the brain for associative learning remain unclear. Here, we report that acute sleep deprivation in *Drosophila* selectively impairs pattern separation—the ability to distinguish between similar stimuli—without affecting classical conditioning. This deficit correlates with disrupted sparse coding in the mushroom body, reflected by an increased number of active Kenyon cells and greater overlap in their odor representations. Electrophysiological analyses reveal that sleep loss enhances small conductance calcium-activated potassium (SK) channel-mediated afterhyperpolarization in GABAergic anterior paired lateral (APL) neurons, leading to reduced levels of feedback inhibition onto Kenyon cells and compromised sparse coding. Targeted knockdown of SK channels in APL neurons reduces their augmented afterhyperpolarization and rescues the pattern separation deficits caused by sleep deprivation. These findings identify a critical role for SK channels in inhibitory interneurons to enable sleep to preserve sparse and decorrelated neural representations, thereby supporting cognitive processes such as pattern separation.

INTRODUCTION

Sleep is essential for various cognitive functions, notably learning and memory.[1–5] While substantial research has elucidated the mechanisms by which post-learning sleep facilitates memory consolidation, the immediate effects of the sleep before learning on subsequent information processing and memory encoding remain less understood. Recent human studies have reported that acute sleep deprivation selectively impairs certain aspects of associative learning. Specifically, it disrupts pattern separation, a neural mechanism that transforms similar or overlapping input patterns into distinct representations—allowing precise discrimination of similar stimuli during associative learning.[6] However, whether such sleep-dependent deficits occur in non-human species is unclear, and the underlying neural mechanisms remain to be elucidated.

Drosophila melanogaster offers a valuable model to investigate these questions. Fly sleep shares many features with mammalian sleep, including its roles in learning and memory.[7–11] Moreover, the fly's mushroom body—a central brain structure involved in learning and memory—employs sparse coding, in which each stimulus activates only a small, distinct subset of neurons.[12–15] This sparse, decorrelated activity pattern minimizes overlap between representations of similar stimuli and enhances pattern separation.[16,17] Thus, this well-characterized neural architecture, combined with the genetic and circuit-level tools available in *Drosophila*, provides a unique opportunity to dissect how sleep loss before learning impacts subsequent information processing and memory formation at behavioral, circuit, and cellular levels.

Here, we report that acute sleep deprivation in *D. melanogaster* selectively impairs pattern separation during associative learning—mirroring results observed in humans. Mechanistically, this deficit stems from sleep-deprivation-driven upregulation of small conductance calcium-activated potassium (SK) channel[18] activity in the γ-aminobutyric acid (GABAergic) anterior paired lateral (APL) neurons, which in turn reduces the levels of feedback inhibition and alters the sparse coding in the mushroom body. Given that sparse coding is a conserved neural coding scheme—employed in regions such as the mammalian cortex,[19–21] hippocampus,[22–26] and insect mushroom body[27,28]—and underlies pattern separation, our findings indicate a broad, evolutionarily conserved mechanism. Specifically, sleep regulates feedback inhibition in neural circuits, tuning the sparsity of representations to support cognitive processes like pattern separation.

Please cite this article in press as: Chen et al., Sleep facilitates pattern separation through SK channel-mediated sparse coding, Current Biology (2026), https://doi.org/10.1016/j.cub.2026.02.028

RESULTS

Acute sleep loss impairs pattern separation in *Drosophila*

To investigate how acute sleep deprivation impacts associative learning, flies were sleep-deprived overnight for 12 h from zeitgeber time (ZT) 12 to ZT24 and tested for their ability to form associations between odor stimuli and electric shocks the following morning. We utilized the individual *Drosophila* olfactory conditioner (iDOC), a single-fly adaptation of the classical T-maze paradigm recently developed in our laboratory,[29] to evaluate associative learning. iDOC, inspired by the original design in Claridge-Chang et al.,[30] enables high-throughput aversive olfactory conditioning and precise measurement of learned performance at the individual fly level. Assessing individual fly performance was critical since sleep monitoring and deprivation were conducted on a per-fly basis, allowing us to directly link sleep metrics with learning performance within the same animal.

We first assessed whether classical olfactory aversive learning remained intact after sleep loss. Flies were given a pre-training choice between an odor stimulus, 3-octanol (OCT), and clean air to measure baseline odor preference. After conditioning, where OCT was paired with electric shock, we retested their odor preference. Both sleep-deprived and control (normal sleep) flies learned to avoid the conditioned stimulus (OCT in this case), showing a significant negative shift in performance index after training (Figures S1A–S1C). These results indicate that acute overnight sleep deprivation does not impair classical Pavlovian learning in *Drosophila*.

Next, we investigated whether acute sleep deprivation affects the ability to discriminate between similar odor mixtures, a behavioral readout of pattern separation. Flies were trained to associate an odor mixture of OCT and methylcyclohexanol (MCH) at a 4:1 ratio (4OCT:1MCH) with electric shock and then assessed with a choice between this mixture and a similar, non-shocked odor mixture (1OCT:4MCH; Figure 1A). Flies with normal sleep successfully learned to avoid the conditioned odor mixture, indicating that they could distinguish between highly similar odor mixtures (Figure 1B). By contrast, sleep-deprived flies failed to show learned avoidance under the same conditions, suggesting impaired discrimination of similar odor stimuli (Figure 1C). Notably, 3 h of recovery sleep following 12 h of sleep loss restored the ability to discriminate these similar odor mixtures (Figure 1D), implying that sleep facilitates pattern separation. To confirm that the observed deficit was due to impaired pattern separation rather than an altered innate preference for specific odor ratios, we performed a reciprocal control experiment. By conditioning flies to the 1OCT:4MCH mixture instead (Figure S1D), we found that sleep-deprived flies still failed to exhibit learned avoidance (Figures S1E and S1F). Consistent with our initial findings, this demonstrates that impairment is independent of the specific odor mixture used as the CS^+. Collectively, these results demonstrate that sleep deprivation impairs odor pattern separation in flies, a deficit that is notably reversed by recovery sleep.

Importantly, the deficit was specific to similar odor discrimination. Sleep-deprived flies trained to discriminate between the 4OCT:1MCH mixture and a chemically distinct odor, pentyl acetate (PA), showed robust learning comparable to flies with normal sleep (Figures 1E–1G). These findings suggest that sleep loss selectively impairs the discrimination of similar odor stimuli in *Drosophila*, mirroring observations in human studies in which sleep deprivation disrupts pattern separation.[6,31]

Leveraging the single-fly resolution of the iDOC system, we next examined the relationship between individual sleep history and learning efficacy. We quantified the total sleep obtained during the 12-h night phase prior to conditioning (Figures S1G and S1H) and analyzed its association with subsequent discrimination performance. For the similar odor discrimination task, linear regression analysis revealed a significant negative association between the amount of night sleep preceding training and changes in performance index (Figure 1H; $p = 0.0375$). Increased sleep was associated with more negative performance indices, whereas sleep-deprived flies clustered near values close to zero, consistent with impaired discrimination of similar odor pairs. By contrast, no significant association was observed between sleep amount and performance in the dissimilar odor discrimination task (Figure 1I; $p = 0.7843$), indicating that the relationship between sleep history and learning performance is selective for pattern separation.

Sleep maintains sparse coding in the mushroom body

In *Drosophila*, the mushroom body employs sparse and decorrelated coding of sensory information, a neural coding scheme critical for similar odor discrimination.[15] Sparse coding ensures that only a limited subset of neurons responds to a given stimulus, and each neuron is activated by only a few stimuli.[20,27] Specifically, for any given odor, ~5%–10% of excitatory principal neurons in the mushroom body, known as Kenyon cells, are activated, and different odors elicit responses in largely non-overlapping Kenyon cell populations.[12,14,15]

Given that acute sleep deprivation impairs pattern separation during associative olfactory learning in flies, we hypothesized that sleep loss would disrupt the sparse coding in the mushroom body. To test this, we expressed the genetically encoded calcium indicator GCaMP6f[32] in all Kenyon cells and performed *in vivo* calcium imaging of Kenyon cell somata in response to a panel of six odors, including odors used in previous behavioral experiments (Figure 2A). Our functional imaging experiments revealed that sleep-deprived flies exhibited a greater number of Kenyon cells responding to each odor compared with control flies with normal sleep (Figure 2B), reflecting a significant reduction in population sparseness following sleep loss (Figure 2D). Importantly, 3 h of recovery sleep following deprivation was sufficient to reverse these effects, restoring population sparseness to levels indistinguishable from normal sleep controls (Figures 2B and 2D).

Furthermore, the similarity of Kenyon cell activation patterns between different odors generally increased after sleep deprivation, as measured by pairwise correlation analyses (Figure 2C). Notably, the similarity between responses to similar odor pairs (4OCT:1MCH and 1OCT:4MCH) was significantly increased in sleep-deprived flies (Figure 2E), whereas recovery sleep restored the decorrelation of the similar odor representations (Figure 2E). Correlations between dissimilar odor pairs (4OCT:1MCH and PA) remained unchanged across all groups (Figure 2F). Collectively, these findings suggest that acute sleep deprivation disrupts both sparse and decorrelated odor

Please cite this article in press as: Chen et al., Sleep facilitates pattern separation through SK channel-mediated sparse coding, Current Biology (2026), https://doi.org/10.1016/j.cub.2026.02.028

CellPress
OPEN ACCESS

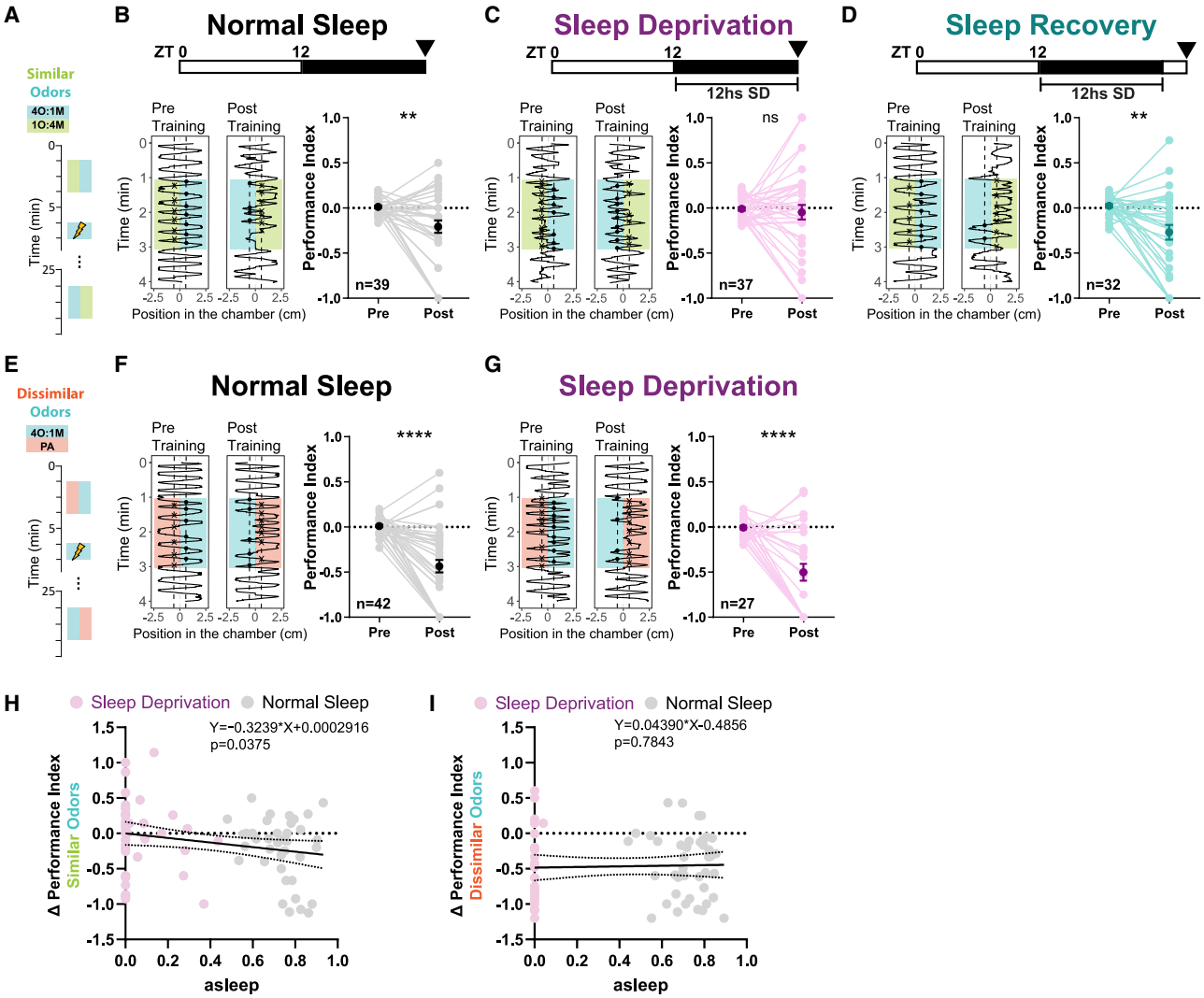

Figure 1. Acute SD impaired learned discrimination of similar but not dissimilar odor pairs

(A) Experimental paradigm illustrating the learned odor discrimination task, comprising pre-training test, aversive conditioning (training), and post-training test phases plotted vertically against time. Colored rectangles indicate odor presentations. For similar odor discrimination, blends of OCT and MCH were used at ratios of 4:1 (4O:1M; CS^+) and 1:4 (1O:4M; CS^-).

(B–D) Discrimination performance for similar odor mixtures. Upper: bars show 12:12 light-dark cycles (white: light, black: dark), zeitgeber time 0 (ZT0) indicates the light on, and arrows indicate the timing of the learned odor discrimination task. Left: representative trajectories of fly positions in the chamber (horizontal dimension) over time (vertical dimension) before and after conditioning. Right: quantification of learning (performance index).

(B) Normal sleep flies (n = 39; p = 0.01) successfully learned to discriminate similar odor mixtures, with the performance index significantly reduced after conditioning.

(C) Sleep-deprived (SD) flies (12 h; n = 37; p = 0.7342) failed discrimination.

(D) Sleep recovery flies (3 h recovery after 12 h deprivation; n = 33; p = 0.0026) regained discrimination.

(E) Experimental paradigm of the dissimilar odor mixture discrimination task, with 4O:1M as CS^+ and PA only as CS^-.

(F and G) Representative trajectories and learning performance quantification are presented similarly as described above. Both (F) the normal sleep (n = 42; $p < 0.0001$) and (G) the SD groups (n = 27; $p < 0.0001$) successfully learn to discriminate the dissimilar odors.

(H and I) Correlation analysis between sleep amount (fraction of time asleep during ZT12–ZT24) and learning performance (Δ performance index) for flies shown in (B), (C), (F), and (G). Solid lines represent linear regression fits, and dashed lines indicate 95% confidence intervals.

(H) For similar odor discrimination (4O:1M vs. 1O:4M), a significant negative association was observed between sleep amount and learning performance (p = 0.0375). The regression line (y = −0.3239x + 0.00029) indicates that increased sleep was associated with more negative performance indices.

(I) For dissimilar odor discrimination (4O:1M vs. PA), no significant association was detected between sleep amount and learning performance (p = 0.7843).

Individual fly performance indices are shown as light-colored dots, and mean values are represented by dark-colored dots. Error bars represent SEM. Statistical significance was examined by the Wilcoxon matched-pairs signed rank test (B–D, F, and G) and linear regression analysis (H and I); ns, not significant; $^*p < 0.05$, $^{**}p < 0.01$, $^{***}p < 0.001$, $^{****}p < 0.0001$.

See also Figure S1.

Please cite this article in press as: Chen et al., Sleep facilitates pattern separation through SK channel-mediated sparse coding, Current Biology (2026), https://doi.org/10.1016/j.cub.2026.02.028

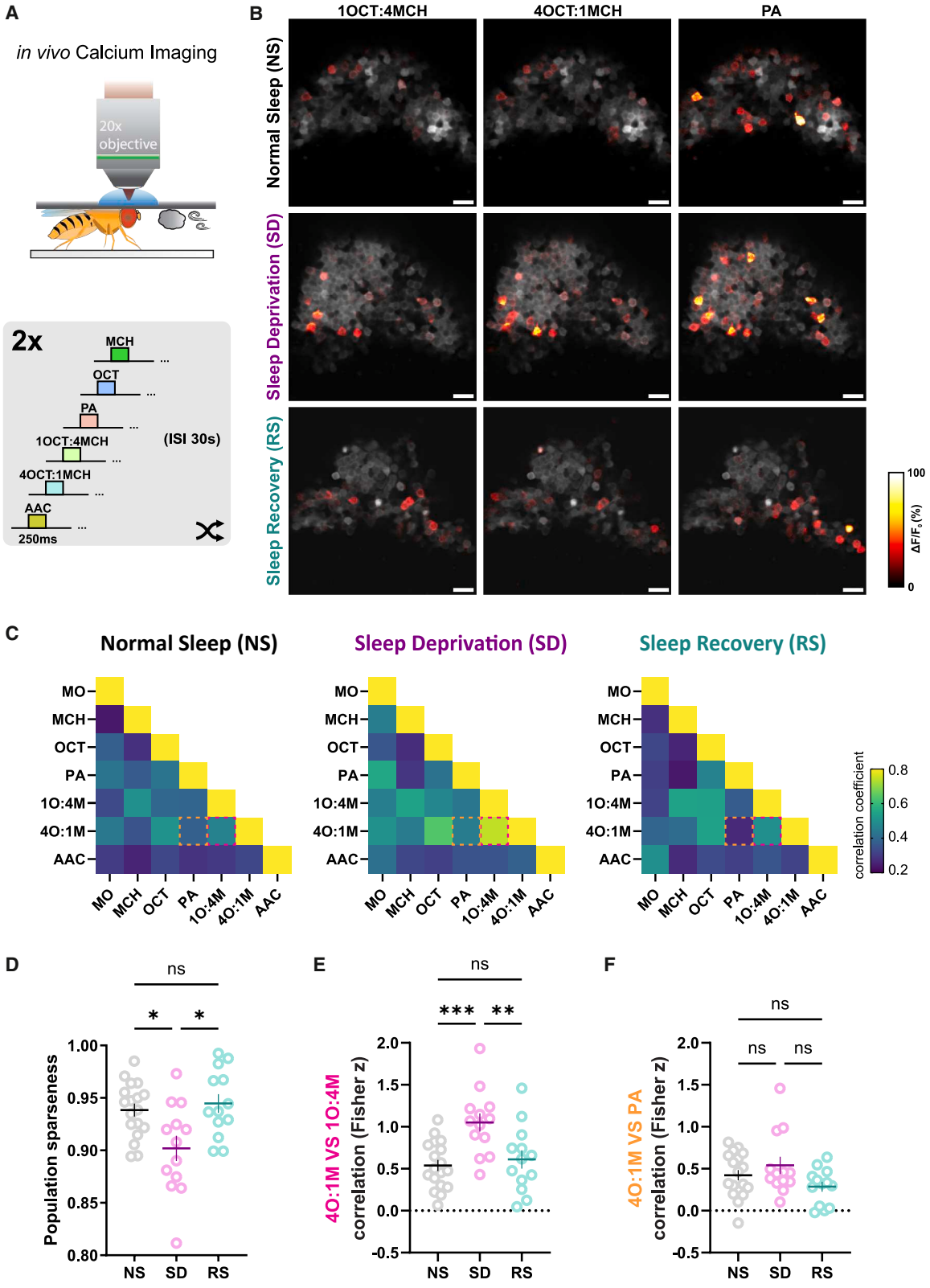

Figure 2. Sleep regulates population sparseness and decorrelation of olfactory representations in the mushroom body

(A) Top: schematic illustrating *in vivo* calcium imaging in flies expressing GCaMP6f in all Kenyon cells using two-photon microscopy. Bottom: experimental paradigm showing repeated application of a randomized sequence of odor stimuli to individual flies, with an inter-stimulus interval (ISI) of 30 s.

(legend continued on next page)

Please cite this article in press as: Chen et al., Sleep facilitates pattern separation through SK channel-mediated sparse coding, Current Biology (2026), https://doi.org/10.1016/j.cub.2026.02.028

representations in the mushroom body, resulting in less distinct neural codes, and that these alterations are reversible with sleep.

Sleep loss enhances SK channel-mediated inhibition in APL neurons

Sparse coding in the mushroom body requires a balance of excitation and inhibition (E/I ratio), with the GABAergic APL neuron providing critical feedback inhibition to excitatory Kenyon cells.[15,33] Given that acute sleep deprivation disrupts sparse coding in the mushroom body, we investigated whether acute sleep loss increases the excitability of Kenyon cells, reduces the inhibitory feedback from APL neurons, or both.

To assess changes in excitability of Kenyon cells, we performed whole-cell patch-clamp recordings on α/β, α′/β′, and γ subtype Kenyon cells from *ex vivo* brain preparations of sleep-deprived and control (normal sleep) flies. Measurements of various membrane properties, including resting membrane potential, input resistance, afterhyperpolarization (AHP) amplitude, membrane time constant, spike threshold, and firing rate in response to current injections, revealed no significant differences between the two groups (Figure 3). These findings indicate that 12 h of acute sleep deprivation does not alter the intrinsic excitability of Kenyon cells.

Next, we examined the electrophysiological properties of inhibitory APL neurons by whole-cell patch-clamp recordings (Figure S2A). Although insect APL neurons were first identified nearly two decades ago,[34,35] no whole-cell patch-clamp recordings had been performed on these cells. Our recordings showed that APL neurons are non-spiking and exhibit graded responses to somatic current injection (Figure 4B). Notably, they display high leak conductance, with input resistance (∼120 MΩ; Figure S2B) nearly two orders of magnitude lower than that of Kenyon cells (∼8–11 GΩ; Figures 3D, 3K, and 3R), consistent with their compartmentalized activity and localized inhibition.[36] In some cases, a spikelet-like "bump" appeared upon strong current injection (Figure 4B), suggesting the presence of voltage-gated channels despite their non-spiking nature.[37,38]

Following 12 h of sleep deprivation, APL neurons show no significant changes in resting membrane potential, input resistance, or the amplitude of the bump or threshold current for bump initiation compared with controls (Figures S2B–S2E). However, sleep-deprived APL neurons exhibited a pronounced increase in AHP amplitude and prolonged AHP decay time following depolarizing current injections (Figures 4C–4E). Crucially, 3 h of recovery sleep following deprivation was sufficient to reverse these defects, restoring both the AHP amplitude and decay kinetics to levels indistinguishable from normal sleep controls (Figures 4C–4E). These findings indicate that APL neurons become more hyperpolarized after activation in sleep-deprived flies, potentially reducing their inhibitory feedback to Kenyon cells and thereby compromising sparse coding in the mushroom body. Importantly, recovery sleep renormalizes this increased AHP, effectively restoring sparse coding.

The enhanced AHP observed in APL neurons after sleep deprivation suggests an upregulation of calcium-activated potassium (K^+) currents. The decay time constant of the enhanced AHP is 491.1 ± 72.17 ms (mean ± SEM), consistent with the kinetics of SK channel-mediated AHP.[39] Thus, the enhanced AHPs in APL neurons after sleep deprivation may be mediated by an increased SK channel activity. To examine this hypothesis, we applied NS8593, a selective SK channel negative modulator,[40] to *ex vivo* brain preparations from sleep-deprived flies. NS8593 abolished the AHP in both conditions (Figure 4F), and the SK-dependent AHP (NS8593-sensitive AHP) was significantly larger in sleep-deprived animals (Figure 4G). Furthermore, RNAi-mediated knockdown of SK channels specifically in APL neurons eliminated the AHP enhancement observed after sleep deprivation (Figures 4H–4J). These pharmacological and genetic experiments confirm that the increased AHP after sleep loss is mediated by the SK channel.

Collectively, these results demonstrate that acute sleep deprivation enhances the conductance of SK channels in APL neurons, leading to increased AHPs, thereby prolonging their refractory period. This change occurs in the absence of alterations in Kenyon cell's excitability or other APL biophysical properties. The enhanced AHP silences APL and reduces inhibitory feedback to excitatory Kenyon cells. This mechanism may underlie the observed disruption of sparse coding in the mushroom body and pattern separation during learning following sleep loss.

Sleep facilitates pattern separation via SK channels in APL neurons

To determine whether SK channels in APL neurons underlie the observed effects of sleep on pattern separation, we examine the ability of flies with SK channel knockdown specifically in APL neurons in the similar odor discrimination task with or without sleep deprivation. Control flies expressing a non-targeting

(B) Representative pseudo-colored calcium response maps in Kenyon cells from normal sleep (NS; top row), sleep deprivation (SD; middle row) flies, and sleep recovery (RS; bottom row) evoked by three odors used in Figure 1: 4O:1M, 4M:1O, and PA, overlaid on grayscale baseline fluorescence images. Scale bar, 10 μm.
(C) Color-coded matrices displaying average pairwise correlations between Kenyon cell response patterns to multiple odors for NS flies (n = 18), SD flies (n = 13), and rebound sleep flies (RS; n = 12). Magenta dashed boxes indicate the inter-odor correlation of similar odor pairs (4O:1M vs. 4M:1O). Orange dashed boxes indicate the inter-odor correlation of dissimilar odor pairs (4O:1M vs. PA).
(D) Quantification of population sparseness averaged across seven olfactory stimuli. SD (n = 13) significantly reduces population sparseness compared with NS (n = 18), while RS (n = 13) restores sparseness to normal levels.
(E) Inter-odor correlation between similar odors (4O:1M vs. 4M:1O) is significantly increased in SD flies (n = 13) compared with NS controls (n = 18). RS (n = 13) restores the decorrelation of similar odors. Each data point represents the Fisher z-transformed Pearson correlation for a given odor pair in an individual fly, lines indicate group means, and error bars represent SEM.
(F) Inter-odor correlation between dissimilar odors (4O:1M vs. PA) remains unchanged across NS (n = 18), SD (n = 13), and RS (n = 13) groups. Each data point represents the Fisher z-transformed Pearson correlation for a given odor pair in an individual fly, lines indicate group means, and error bars represent SEM.
Statistical significance was examined by the Kruskal-Wallis test followed by Dunn's multiple comparisons test (D). For each odor pair, Fisher z-transformed Pearson correlation coefficients were compared across sleep conditions using ordinary one-way ANOVA followed by Tukey's multiple comparisons test (E and F); ns, not significant; $^*p < 0.05$, $^{**}p < 0.01$, $^{***}p < 0.001$.

Please cite this article in press as: Chen et al., Sleep facilitates pattern separation through SK channel-mediated sparse coding, Current Biology (2026), https://doi.org/10.1016/j.cub.2026.02.028

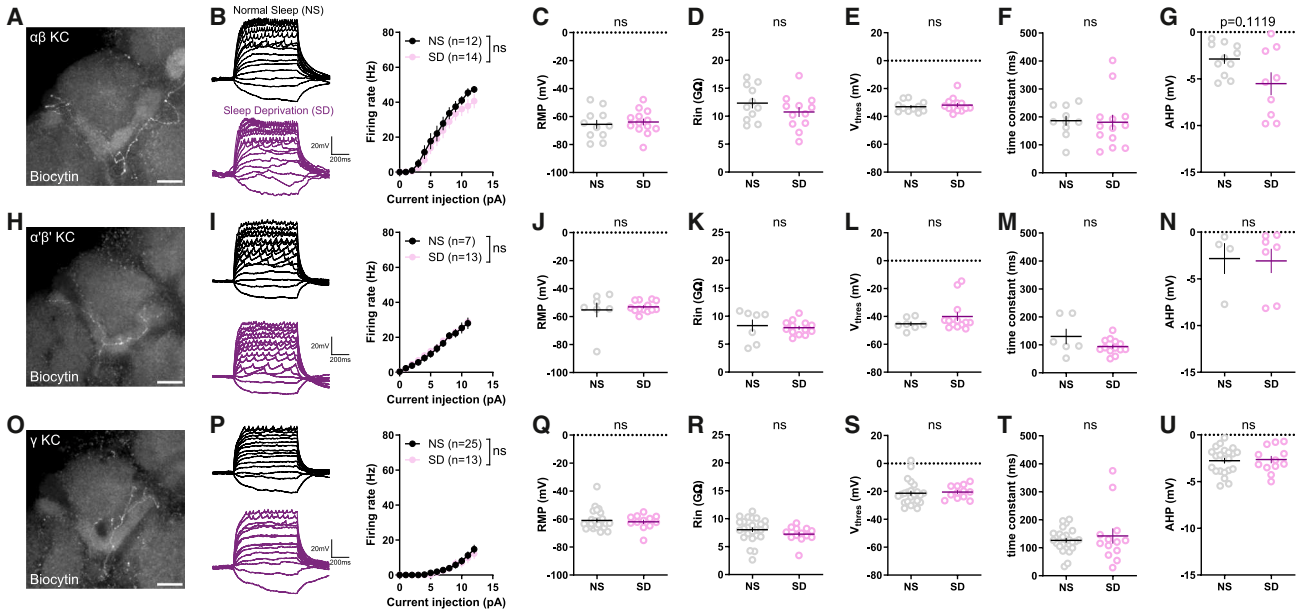

Figure 3. Sleep deprivation does not alter the intrinsic electrical properties of KCs

(A–G) Intrinsic membrane properties of αβ Kenyon cells (KCs) under normal sleep (NS) and sleep deprivation (SD) conditions.

(A) Post hoc immunohistochemistry of a representative biocytin-filled αβ KC. Scale bar, 20 μm.

(B) Left: representative voltage traces from αβ KCs in NS (black) and SD (magenta) flies in response to current steps (−1 to 12 pA). Right: current-firing-rate relationships show no significant difference between groups (NS, $n = 12$; SD, $n = 14$).

(C–G) Quantification of resting membrane potential (RMP; NS, $n = 11$; SD, $n = 12$; C), input resistance (R_{in}; NS, $n = 11$; SD, $n = 12$; D), spike threshold (V_{thres}; NS, $n = 11$; SD, $n = 12$; E), membrane time constant (NS, $n = 10$; SD, $n = 12$; F), and afterhyperpolarization (AHP) amplitude (NS, $n = 11$; SD, $n = 8$; G) reveals no significant differences ($p = 0.1119$ for AHP).

(H–N) Intrinsic membrane properties of α′β′ KCs under NS ($n = 7$) and SD ($n = 13$) conditions.

(H) Post hoc immunohistochemistry of a representative biocytin-filled α′β′ KC. Scale bar, 20 μm.

(I) Left: representative firing responses to current steps in NS and SD flies; right: no significant difference in current-firing-rate curves.

(J–N) No significant differences were observed in RMP (NS, $n = 7$; SD, $n = 13$; J), R_{in} (NS, $n = 7$; SD, $n = 13$; K), V_{thres} (NS, $n = 7$; SD, $n = 13$; L), membrane time constant (NS, $n = 6$; SD, $n = 13$; M), or AHP amplitude (NS, $n = 4$; SD, $n = 7$; N).

(O–U) Intrinsic membrane properties of γ KCs under NS ($n = 25$) and SD ($n = 13$) conditions.

(O) Post hoc staining of a representative biocytin-filled γ KC. Scale bar, 20 μm.

(P) Left: representative voltage responses to current injections; right: no significant difference in firing rate across conditions.

(Q–U) RMP (NS, $n = 25$; SD, $n = 12$; Q), R_{in} (NS, $n = 25$; SD, $n = 13$; R), V_{thres} (NS, $n = 23$; SD, $n = 12$; S), membrane time constant (NS, $n = 25$; SD, $n = 13$; T), and AHP amplitude (NS, $n = 22$; SD, $n = 12$; U) were not significantly different between NS and SD groups.

Data are presented as mean ± SEM. Individual data points are shown. Statistical comparisons were performed using the Mann-Whitney test. ns, not significant.

RNAi exhibited normal discrimination of similar odor mixtures under baseline sleep conditions but failed to discriminate the same odors following sleep deprivation (Figures 5A and 5B), consistent with prior observations (Figures 1B and 1C). By contrast, flies with SK channel knockdown specifically in APL neurons maintained their ability to discriminate between similar odors even after sleep deprivation (Figures 5C and 5D). These results indicate that the suppression of the SK channel specifically in APL neurons mitigates the detrimental effects of sleep loss on pattern separation.

DISCUSSION

Sleep loss impairs pattern separation, an effect observed in human studies[6,31] but not reported in non-human animals. In this study, we found that one night of sleep deprivation impairs pattern separation in an associative learning task while leaving Pavlovian learning intact in fruit flies. This implies an evolutionarily conserved function of sleep on specific aspects of cognitive functions. Mechanistically, we discovered that sleep loss significantly enhances the amplitude and duration of the AHP in GABAergic APL neurons—an alteration we confirmed to be mediated by SK channels through pharmacological and genetic manipulations. This augmented AHP likely prolongs the refractory period of APL neurons, thereby dampening their ability to provide sustained feedback inhibition onto excitatory Kenyon cells. This reduction in feedback inhibition compromises sparse coding within the mushroom body, impairing pattern separation during associative learning. These findings highlight a mechanistic link between sleep, SK channel activity in inhibitory neurons, neural coding strategies such as sparse coding, and the preservation of cognitive functions, including pattern separation.

The inhibitory APL neuron functions as a critical hub for regulating olfactory learning and memory in *Drosophila*. Previous studies have established that APL neurons constrain learning through broad feedback inhibition—acting as a "brake" that is transiently released by dopaminergic suppression during

Please cite this article in press as: Chen et al., Sleep facilitates pattern separation through SK channel-mediated sparse coding, Current Biology (2026), https://doi.org/10.1016/j.cub.2026.02.028

CellPress
OPEN ACCESS

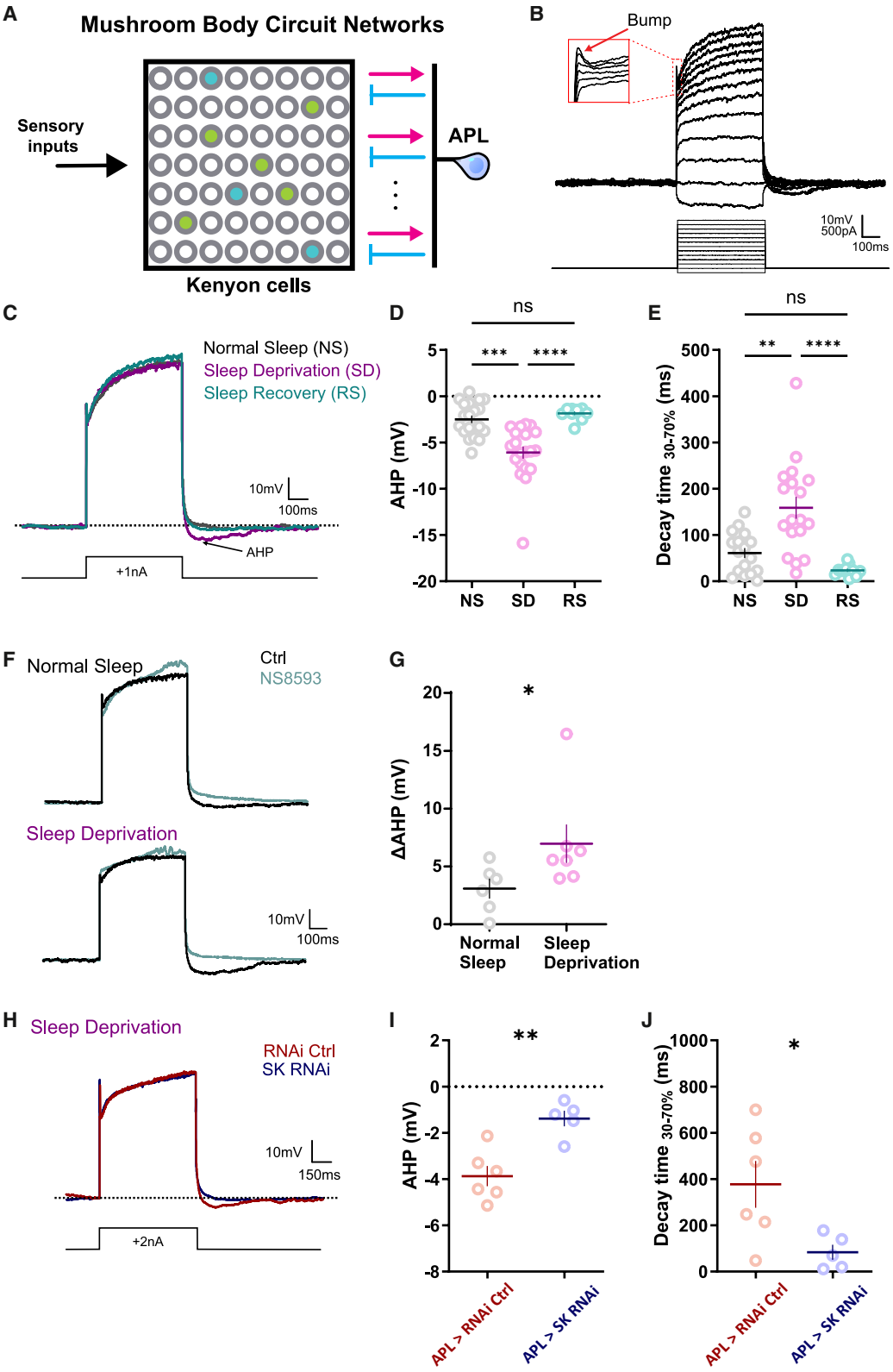

Figure 4. Sleep deprivation enhances and recovery sleep reduces SK channel-mediated AHP in APL neurons in the mushroom body

(A) Schematic illustrating the mushroom body circuit network, highlighting the local feedback inhibition between excitatory Kenyon cells and the inhibitory anterior paired lateral (APL) neuron.

(legend continued on next page)

Please cite this article in press as: Chen et al., Sleep facilitates pattern separation through SK channel-mediated sparse coding, Current Biology (2026), https://doi.org/10.1016/j.cub.2026.02.028

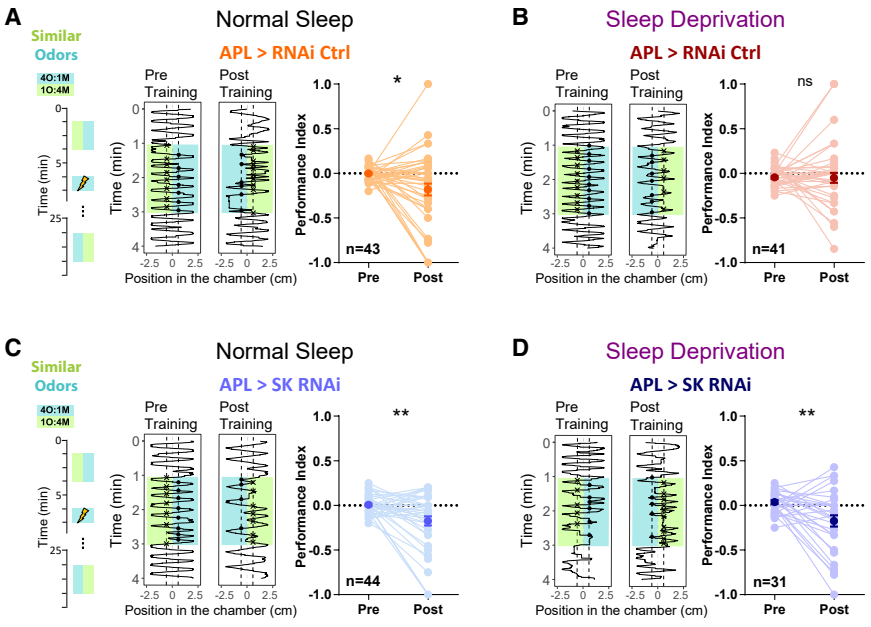

Figure 5. SK channel knockdown in APL neurons rescues sleep loss-induced deficits in learned discrimination of similar odors

Odor discrimination learning performance for the similar odor pair (4O:1M vs. 1O:4M) was assessed in flies expressing control RNAi (*APL > RNAi Ctrl*) or SK RNAi (*APL > SK RNAi*) specifically in APL neurons under conditions of normal sleep and 12 h sleep deprivation.

(A) Representative trajectories (left) illustrate fly positions within the chamber (horizontal dimension) over time (vertical dimension). Performance indices (right) pre- and post-training of *APL > RNAi Ctrl* flies under normal sleep conditions ($n = 43$, $p = 0.0302$) indicate successful learning discrimination.

(B) Sleep-deprived *APL > RNAi Ctrl* flies ($n = 41$, $p = 0.8366$) failed to discriminate the similar odor mixtures, as indicated by no significant difference in performance index post-training.

(C) *APL > SK RNAi* flies under normal sleep conditions ($n = 44$, $p = 0.0041$) exhibited significant learning discrimination of similar odors.

(D) Sleep-deprived *APL > SK RNAi* flies ($n = 31$, $p = 0.0051$) retained their ability to discriminate similar odors.

Individual fly performance indices are shown as light-colored dots, and mean values are represented by dark-colored dots. Error bars represent SEM. Statistical significance was examined by the Wilcoxon matched-pairs signed rank test; ns, not significant; $^{*}p < 0.05$, $^{**}p < 0.01$.

memory formation to facilitate encoding.[35,41] Beyond initial acquisition, APL neurons are also implicated in reversal, highlighting their multifaceted role in cognitive flexibility and stability.[42,43] Here, we demonstrate that sleep deprivation prior to learning specifically targets this feedback inhibition, enhancing the AHP in APL neurons and impairing pattern separation. We propose that by tuning this APL-dependent inhibition, sleep sets the optimal activity for the entire mushroom body circuit. This regulation likely extends beyond the encoding phase: just as pre-learning sleep primes the network for pattern separation, post-learning sleep may utilize this same mechanism—renormalizing APL excitability—to facilitate memory consolidation and flexible updating. Thus, the sleep-dependent modulation of APL inhibition likely represents a convergent mechanism through which sleep history influences a broad spectrum of cognitive capabilities.

Our findings position the APL neuron within a mushroom body network where multiple elements regulate both sleep and memory. Unlike dopaminergic neurons,[44,45] Kenyon cells,[46–48] and dorsal paired medial (DPM) neurons, which actively regulate sleep states alongside their memory functions, the APL neuron appears to play a minor role in sleep regulation. Despite electrical coupling to sleep-promoting DPMs,[49] APL inhibition yields only weak effects on sleep.[50] Therefore, our results suggest a functional division of labor where APL neurons serve as a primary target rather than a regulator of sleep.

Our study demonstrates that sleep and wakefulness specifically modulate the AHP of the inhibitory APL neuron, without broadly altering the intrinsic excitability of excitatory Kenyon cells. These observations indicate a disruption in the E/I ratio in the mushroom body network following sleep loss. This is consistent with recent findings in the mammalian visual cortex, where the feedback inhibition pathway exhibits daily oscillations and is upregulated in the morning after wakefulness at night, whereas feedforward inhibition pathways show no

(B) Representative current-clamp recordings show the discharge pattern of APL neurons (top) in response to current steps (bottom). The recorded APL neuron manifests a non-spiking property but exhibits initial membrane bumps upon strong depolarization (red inset).

(C) Representative traces of AHP responses in APL neurons following 1 nA current injection after 12 h of sleep deprivation (SD) compared with normal sleep (NS) and sleep recovery (RS) conditions.

(D) Quantification of AHP magnitude shows a significant increase in SD flies ($n = 20$) compared with those with NS ($n = 20$) and with rebound sleep (RS; $n = 11$).

(E) Quantification of AHP decay time (30%–70%), significantly prolonged in SD flies ($n = 18$) compared with NS flies ($n = 17$) and RS flies ($n = 11$).

(F and G) Representative traces (F) and quantification (G) of AHP amplitude changes (ΔAHP; amplitude difference before and after treatment) induced by NS8593, an SK channel negative modulator. SD flies ($n = 7$) showed significantly greater ΔAHP compared with NS flies ($n = 6$), indicating that AHP enhancement by SD was largely SK channel-mediated.

(H–J) Effects of APL-specific SK channel knockdown (*APL > SK RNAi*) on AHP responses following 12-h SD. Representative traces (H), AHP amplitude quantification (I), and AHP decay time quantification (J) in APL-specific SK knockdown flies (*APL > SK RNAi*, $n = 5$) compared with RNAi control flies (*APL > RNAi Ctrl*, $n = 6$). APL-specific SK knockdown significantly reduced AHP amplitude and decay time following SD.

Data are presented as mean ± SEM. Individual data points are shown. Statistical significance was examined by the Kruskal-Wallis test followed by Dunn's multiple comparisons test (D and E) and by the Mann-Whitney test (G, I, and J); ns, not significant; $^{*}p < 0.05$, $^{**}p < 0.01$, $^{***}p < 0.001$, $^{****}p < 0.0001$.

See also Figure S2.

significant changes.[51] Similarly, the APL neuron in the fly mushroom body network provides feedback inhibition,[15,36] suggesting that sleep's role in maintaining feedback inhibition in neural networks is evolutionarily conserved. Although the functional consequences of sleep-dependent increases in feedback inhibition in the mammalian cortex have remained unclear, our observations provide insights into this issue. Because sparse coding is also employed in mammals, it is likely that acute sleep loss disrupts sparse coding in multiple brain areas, impairing various cognitive functions that rely on sparse coding.

SK channels are known to play a critical role in sleep regulation, particularly in maintaining low-frequency brain oscillations in mammals.[52] Studies have shown that SK2 knockout mice exhibit disrupted thalamic-cortical oscillations and fragmented sleep, underscoring their role in stabilizing sleep architecture.[53] Here, we demonstrate that sleep and wakefulness regulate the SK channel-mediated AHP in GABAergic interneurons. This suggests a bidirectional relationship in which reduced SK channel function impairs sleep, while excessive SK channel activity during wakefulness disrupts cognitive processes such as pattern separation. Understanding how sleep and wakefulness regulate SK channel activity at optimal levels in different cell types is an important question for future research.

RESOURCE AVAILABILITY

Lead contact

Requests for further information and resources should be directed to, and will be fulfilled by, the lead contact, Sha Liu (sha.liu@kuleuven.be).

Materials availability

Fly lines generated in this study are available upon request from the lead contact.

Data and code availability

- This paper did not generate any original code.
- Raw data for imaging, electrophysiology, and behavioral experiments have been deposited at Zenodo: https://doi.org/10.5281/zenodo.18644411.
- Any additional information required to reanalyze the data reported in this paper is available from the lead contact upon request.

ACKNOWLEDGMENTS

We thank the Bloomington Drosophila Stock Center (supported by NIH P40OD018537), the Vienna Drosophila Resource Center (VDRC), and Dr. Gerald M. Rubin for providing the fly stocks. This research was supported by the European Research Council (StG 758580 to S.L.) and the Fonds voor Wetenschappelijk Onderzoek (FWO) Research Project (G052922N to S.L.).

AUTHOR CONTRIBUTIONS

Conceptualization, C.-C.C. and S.L.; data curation, C.-C.C. and Y.-C.H.; formal analysis, C.-C.C., Y.-C.H., and A.O.; funding acquisition, S.L.; methodology, C.-C.C., A.O., E.T., E.-S.B., Y.W., A.C.L., and S.L.; project administration, S.L.; resources, C.-C.C., R.S.-G., A.C.L., and S.L.; supervision, S.L.; visualization, C.-C.C. and S.L.; writing – original draft, C.-C.C. and S.L.; writing – review and editing, C.-C.C., R.S.-G., A.C.L., and S.L.

DECLARATION OF INTERESTS

The authors declare no competing interests.

STAR★METHODS

Detailed methods are provided in the online version of this paper and include the following:

- KEY RESOURCES TABLE
- EXPERIMENTAL MODEL AND STUDY PARTICIPANT DETAILS
  - Fly husbandry
  - Fly strains
- METHOD DETAILS
  - Sleep behavior and sleep deprivation
  - Learning behavior of individual flies
  - *In vivo* Calcium imaging
  - Odor stimulation
  - Electrophysiological recordings
  - Immunofluorescence and confocal imaging
- QUANTIFICATION AND STATISTICAL ANALYSIS
  - Image processing and analysis
  - Population sparseness
  - Inter-Odor correlation
  - Statistical analyses

SUPPLEMENTAL INFORMATION

Supplemental information can be found online at https://doi.org/10.1016/j.cub.2026.02.028.

Received: August 29, 2025
Revised: February 10, 2026
Accepted: February 16, 2026

REFERENCES

1. Yoo, S.-S., Hu, P.T., Gujar, N., Jolesz, F.A., and Walker, M.P. (2007). A deficit in the ability to form new human memories without sleep. Nat. Neurosci. *10*, 385–392. https://doi.org/10.1038/nn1851.
2. Mander, B.A., Santhanam, S., Saletin, J.M., and Walker, M.P. (2011). Wake deterioration and sleep restoration of human learning. Curr. Biol. *21*, R183–R184. https://doi.org/10.1016/j.cub.2011.01.019.
3. Diekelmann, S., and Born, J. (2010). The memory function of sleep. Nat. Rev. Neurosci. *11*, 114–126. https://doi.org/10.1038/nrn2762.
4. Rasch, B., and Born, J. (2013). About sleep's role in memory. Physiol. Rev. *93*, 681–766. https://doi.org/10.1152/physrev.00032.2012.
5. Vorster, A.P., and Born, J. (2015). Sleep and memory in mammals, birds and invertebrates. Neurosci. Biobehav. Rev. *50*, 103–119. https://doi.org/10.1016/j.neubiorev.2014.09.020.
6. Saletin, J.M., Goldstein-Piekarski, A.N., Greer, S.M., Stark, S., Stark, C.E., and Walker, M.P. (2016). Human hippocampal structure: a novel biomarker predicting mnemonic vulnerability to, and recovery from, sleep deprivation. J. Neurosci. *36*, 2355–2363. https://doi.org/10.1523/JNEUROSCI.3466-15.2016.
7. Donlea, J.M., Thimgan, M.S., Suzuki, Y., Gottschalk, L., and Shaw, P.J. (2011). Inducing sleep by remote control facilitates memory consolidation in Drosophila. Science *332*, 1571–1576. https://doi.org/10.1126/science.1202249.
8. Chouhan, N.S., Griffith, L.C., Haynes, P., and Sehgal, A. (2021). Availability of food determines the need for sleep in memory consolidation. Nature *589*, 582–585. https://doi.org/10.1038/s41586-020-2997-y.
9. Melnattur, K., Kirszenblat, L., Morgan, E., Militchin, V., Sakran, B., English, D., Patel, R., Chan, D., van Swinderen, B., and Shaw, P.J. (2021). A conserved role for sleep in supporting spatial learning in Drosophila. Sleep *44*, zsaa197. https://doi.org/10.1093/sleep/zsaa197.

10. Dissel, S. (2020). Drosophila as a model to study the relationship between sleep, plasticity, and memory. Front. Physiol. *11*, 533. https://doi.org/10.3389/fphys.2020.00533.

11. Marquand, K., Roselli, C., Cervantes-Sandoval, I., and Boto, T. (2023). Sleep benefits different stages of memory in Drosophila. Front. Physiol. *14*, 1087025. https://doi.org/10.3389/fphys.2023.1087025.

12. Turner, G.C., Bazhenov, M., and Laurent, G. (2008). Olfactory representations by Drosophila mushroom body neurons. J. Neurophysiol. *99*, 734–746. https://doi.org/10.1152/jn.01283.2007.

13. Murthy, M., Fiete, I., and Laurent, G. (2008). Testing odor response stereotypy in the Drosophila mushroom body. Neuron *59*, 1009–1023. https://doi.org/10.1016/j.neuron.2008.07.040.

14. Honegger, K.S., Campbell, R.A.A., and Turner, G.C. (2011). Cellular-resolution population imaging reveals robust sparse coding in the Drosophila mushroom body. J. Neurosci. *31*, 11772–11785. https://doi.org/10.1523/JNEUROSCI.1099-11.2011.

15. Lin, A.C., Bygrave, A.M., de Calignon, A., Lee, T., and Miesenböck, G. (2014). Sparse, decorrelated odor coding in the mushroom body enhances learned odor discrimination. Nat. Neurosci. *17*, 559–568. https://doi.org/10.1038/nn.3660.

16. Cayco-Gajic, N.A., Clopath, C., and Silver, R.A. (2017). Sparse synaptic connectivity is required for decorrelation and pattern separation in feedforward networks. Nat. Commun. *8*, 1116. https://doi.org/10.1038/s41467-017-01109-y.

17. Cayco-Gajic, N.A., and Silver, R.A. (2019). Re-evaluating circuit mechanisms underlying pattern separation. Neuron *101*, 584–602. https://doi.org/10.1016/j.neuron.2019.01.044.

18. Adelman, J.P., Maylie, J., and Sah, P. (2012). Small-conductance Ca2+-activated K+ channels: form and function. Annu. Rev. Physiol. *74*, 245–269. https://doi.org/10.1146/annurev-physiol-020911-153336.

19. Rolls, E.T., and Tovee, M.J. (1995). Sparseness of the neuronal representation of stimuli in the primate temporal visual cortex. J. Neurophysiol. *73*, 713–726. https://doi.org/10.1152/jn.1995.73.2.713.

20. Vinje, W.E., and Gallant, J.L. (2000). Sparse coding and decorrelation in primary visual cortex during natural vision. Science *287*, 1273–1276. https://doi.org/10.1126/science.287.5456.1273.

21. Willmore, B.D.B., Mazer, J.A., and Gallant, J.L. (2011). Sparse coding in striate and extrastriate visual cortex. J. Neurophysiol. *105*, 2907–2919. https://doi.org/10.1152/jn.00594.2010.

22. Chawla, M.K., Guzowski, J.F., Ramirez-Amaya, V., Lipa, P., Hoffman, K.L., Marriott, L.K., Worley, P.F., McNaughton, B.L., and Barnes, C.A. (2005). Sparse, environmentally selective expression of Arc RNA in the upper blade of the rodent fascia dentata by brief spatial experience. Hippocampus *15*, 579–586. https://doi.org/10.1002/hipo.20091.

23. Tashiro, A., Makino, H., and Gage, F.H. (2007). Experience-specific functional modification of the dentate gyrus through adult neurogenesis: a critical period during an immature stage. J. Neurosci. *27*, 3252–3259. https://doi.org/10.1523/JNEUROSCI.4941-06.2007.

24. GoodSmith, D., Chen, X., Wang, C., Kim, S.H., Song, H., Burgalossi, A., Christian, K.M., and Knierim, J.J. (2017). Spatial representations of granule cells and mossy cells of the dentate gyrus. Neuron *93*, 677–690.e5. https://doi.org/10.1016/j.neuron.2016.12.026.

25. Senzai, Y., and Buzsáki, G. (2017). Physiological properties and behavioral correlates of hippocampal granule cells and mossy cells. Neuron *93*, 691–704.e5. https://doi.org/10.1016/j.neuron.2016.12.011.

26. Danielson, N.B., Turi, G.F., Ladow, M., Chavlis, S., Petrantonakis, P.C., Poirazi, P., and Losonczy, A. (2017). In vivo imaging of dentate gyrus mossy cells in behaving mice. Neuron *93*, 552–559.e4. https://doi.org/10.1016/j.neuron.2016.12.019.

27. Perez-Orive, J., Mazor, O., Turner, G.C., Cassenaer, S., Wilson, R.I., and Laurent, G. (2002). Oscillations and sparsening of odor representations in the mushroom body. Science *297*, 359–365. https://doi.org/10.1126/science.1070502.

28. Broome, B.M., Jayaraman, V., and Laurent, G. (2006). Encoding and decoding of overlapping odor sequences. Neuron *51*, 467–482. https://doi.org/10.1016/j.neuron.2006.07.018.

29. Ortega, A., Tedre, E., Baz, E.-S., Tsao, C.-H., Chen, C.-C., and Liu, S. (2024). A high-throughput platform for assessing single fly learning and memory: Individual *Drosophila* olfactory conditioner (iDOC). Preprint at bioRxiv. https://doi.org/10.1101/2024.12.18.629135.

30. Claridge-Chang, A., Roorda, R.D., Vrontou, E., Sjulson, L., Li, H., Hirsh, J., and Miesenböck, G. (2009). Writing memories with light-addressable reinforcement circuitry. Cell *139*, 405–415. https://doi.org/10.1016/j.cell.2009.08.034.

31. Blokland, A., Jackson, M., Puustinen, K., Soeterboek, J., and Heckman, P.R.A. (2024). Acute sleep loss impairs object but not spatial pattern separation in humans. Neurosci. Lett. *818*, 137535. https://doi.org/10.1016/j.neulet.2023.137535.

32. Chen, T.-W., Wardill, T.J., Sun, Y., Pulver, S.R., Renninger, S.L., Baohan, A., Schreiter, E.R., Kerr, R.A., Orger, M.B., Jayaraman, V., et al. (2013). Ultrasensitive fluorescent proteins for imaging neuronal activity. Nature *499*, 295–300. https://doi.org/10.1038/nature12354.

33. Papadopoulou, M., Cassenaer, S., Nowotny, T., and Laurent, G. (2011). Normalization for sparse encoding of odors by a wide-field interneuron. Science *332*, 721–725. https://doi.org/10.1126/science.1201835.

34. Tanaka, N.K., Tanimoto, H., and Ito, K. (2008). Neuronal assemblies of the Drosophila mushroom body. J. Comp. Neurol. *508*, 711–755. https://doi.org/10.1002/cne.21692.

35. Liu, X., and Davis, R.L. (2009). The GABAergic anterior paired lateral neuron suppresses and is suppressed by olfactory learning. Nat. Neurosci. *12*, 53–59. https://doi.org/10.1038/nn.2235.

36. Amin, H., Apostolopoulou, A.A., Suárez-Grimalt, R., Vrontou, E., and Lin, A.C. (2020). Localized inhibition in the Drosophila mushroom body. eLife *9*, e56954. https://doi.org/10.7554/eLife.56954.

37. De Biase, L.M., Nishiyama, A., and Bergles, D.E. (2010). Excitability and synaptic communication within the oligodendrocyte lineage. J. Neurosci. *30*, 3600–3611. https://doi.org/10.1523/JNEUROSCI.6000-09.2010.

38. Chittajallu, R., Aguirre, A., and Gallo, V. (2004). NG2-positive cells in the mouse white and grey matter display distinct physiological properties. J. Physiol. *561*, 109–122. https://doi.org/10.1113/jphysiol.2004.074252.

39. Stocker, M. (2004). Ca(2+)-activated K+ channels: molecular determinants and function of the SK family. Nat. Rev. Neurosci. *5*, 758–770. https://doi.org/10.1038/nrn1516.

40. Strøbaek, D., Hougaard, C., Johansen, T.H., Sørensen, U.S., Nielsen, E.Ø., Nielsen, K.S., Taylor, R.D.T., Pedarzani, P., and Christophersen, P. (2006). Inhibitory gating modulation of small conductance Ca2+-activated K+ channels by the synthetic compound (R)-N-(benzimidazol-2-yl)-1,2,3,4-tetrahydro-1-naphtylamine (NS8593) reduces afterhyperpolarizing current in hippocampal CA1 neurons. Mol. Pharmacol. *70*, 1771–1782. https://doi.org/10.1124/mol.106.027110.

41. Zhou, M., Chen, N., Tian, J., Zeng, J., Zhang, Y., Zhang, X., Guo, J., Sun, J., Li, Y., Guo, A., et al. (2019). Suppression of GABAergic neurons through D2-like receptor secures efficient conditioning in Drosophila aversive olfactory learning. Proc. Natl. Acad. Sci. USA *116*, 5118–5125. https://doi.org/10.1073/pnas.1812342116.

42. Ren, Q., Li, H., Wu, Y., Ren, J., and Guo, A. (2012). A GABAergic inhibitory neural circuit regulates visual reversal learning in Drosophila. J. Neurosci. *32*, 11524–11538. https://doi.org/10.1523/JNEUROSCI.0827-12.2012.

43. Wu, Y., Ren, Q., Li, H., and Guo, A. (2012). The GABAergic anterior paired lateral neurons facilitate olfactory reversal learning in Drosophila. Learn. Mem. *19*, 478–486. https://doi.org/10.1101/lm.025726.112.

44. Driscoll, M., Buchert, S.N., Coleman, V., McLaughlin, M., Nguyen, A., and Sitaraman, D. (2021). Compartment specific regulation of sleep by mushroom body requires GABA and dopaminergic signaling. Sci. Rep. *11*, 20067. https://doi.org/10.1038/s41598-021-99531-2.

45. Sitaraman, D., Aso, Y., Rubin, G.M., and Nitabach, M.N. (2015). Control of sleep by dopaminergic inputs to the Drosophila mushroom body. Front. Neural Circuits *9*, 73. https://doi.org/10.3389/fncir.2015.00073.

46. Pitman, J.L., McGill, J.J., Keegan, K.P., and Allada, R. (2006). A dynamic role for the mushroom bodies in promoting sleep in Drosophila. Nature *441*, 753–756. https://doi.org/10.1038/nature04739.

47. Joiner, W.J., Crocker, A., White, B.H., and Sehgal, A. (2006). Sleep in Drosophila is regulated by adult mushroom bodies. Nature *441*, 757–760. https://doi.org/10.1038/nature04811.

48. Sitaraman, D., Aso, Y., Jin, X., Chen, N., Felix, M., Rubin, G.M., and Nitabach, M.N. (2015). Propagation of homeostatic sleep signals by segregated synaptic microcircuits of the Drosophila mushroom body. Curr. Biol. *25*, 2915–2927. https://doi.org/10.1016/j.cub.2015.09.017.

49. Wu, C.-L., Shih, M.-F.M., Lai, J.S.-Y., Yang, H.-T., Turner, G.C., Chen, L., and Chiang, A.-S. (2011). Heterotypic gap junctions between two neurons in the Drosophila brain are critical for memory. Curr. Biol. *21*, 848–854. https://doi.org/10.1016/j.cub.2011.02.041.

50. Haynes, P.R., Christmann, B.L., and Griffith, L.C. (2015). A single pair of neurons links sleep to memory consolidation in Drosophila melanogaster. eLife *4*, e03868. https://doi.org/10.7554/eLife.03868.

51. Bridi, M.C.D., Zong, F.-J., Min, X., Luo, N., Tran, T., Qiu, J., Severin, D., Zhang, X.-T., Wang, G., Zhu, Z.-J., et al. (2020). Daily oscillation of the excitation-inhibition balance in visual cortical circuits. Neuron *105*, 621–629.e4. https://doi.org/10.1016/j.neuron.2019.11.011.

52. Cueni, L., Canepari, M., Luján, R., Emmenegger, Y., Watanabe, M., Bond, C.T., Franken, P., Adelman, J.P., and Lüthi, A. (2008). T-type Ca2+ channels, SK2 channels and SERCAs gate sleep-related oscillations in thalamic dendrites. Nat. Neurosci. *11*, 683–692. https://doi.org/10.1038/nn.2124.

53. Wimmer, R.D., Astori, S., Bond, C.T., Rovó, Z., Chatton, J.-Y., Adelman, J.P., Franken, P., and Lüthi, A. (2012). Sustaining sleep spindles through enhanced SK2-channel activity consolidates sleep and elevates arousal threshold. J. Neurosci. *32*, 13917–13928. https://doi.org/10.1523/JNEUROSCI.2313-12.2012.

54. Walcott, K.C.E., Mauthner, S.E., Tsubouchi, A., Robertson, J., and Tracey, W.D. (2018). The Drosophila small conductance calcium-activated potassium channel negatively regulates nociception. Cell Rep. *24*, 3125–3132.e3. https://doi.org/10.1016/j.celrep.2018.08.070.

55. Pfeiffer, B.D., Ngo, T.-T.B., Hibbard, K.L., Murphy, C., Jenett, A., Truman, J.W., and Rubin, G.M. (2010). Refinement of tools for targeted gene expression in Drosophila. Genetics *186*, 735–755. https://doi.org/10.1534/genetics.110.119917.

56. Geissmann, Q., Garcia Rodriguez, L., Beckwith, E.J., French, A.S., Jamasb, A.R., and Gilestro, G.F. (2017). Ethoscopes: An open platform for high-throughput ethomics. PLoS Biol. *15*, e2003026. https://doi.org/10.1371/journal.pbio.2003026.

57. Dopp, J., Ortega, A., Davie, K., Poovathingal, S., Baz, E.-S., and Liu, S. (2024). Single-cell transcriptomics reveals that glial cells integrate homeostatic and circadian processes to drive sleep-wake cycles. Nat. Neurosci. *27*, 359–372. https://doi.org/10.1038/s41593-023-01549-4.

58. Geissmann, Q., Garcia Rodriguez, L., Beckwith, E.J., and Gilestro, G.F. (2019). Rethomics: An R framework to analyse high-throughput behavioural data. PLoS One *14*, e0209331. https://doi.org/10.1371/journal.pone.0209331.

59. Stopfer, M., and Laurent, G. (1999). Short-term memory in olfactory network dynamics. Nature *402*, 664–668. https://doi.org/10.1038/45244.

60. Goodman, M.B., and Lockery, S.R. (2000). Pressure polishing: a method for re-shaping patch pipettes during fire polishing. J. Neurosci. Methods *100*, 13–15. https://doi.org/10.1016/S0165-0270(00)00224-7.

61. Johnson, B.E., Brown, A.L., and Goodman, M.B. (2008). Pressure-polishing pipettes for improved patch-clamp recording. J. Vis. Exp. *20*, 964. https://doi.org/10.3791/964.

62. Abou Tayoun, A.N., Li, X., Chu, B., Hardie, R.C., Juusola, M., and Dolph, P.J. (2011). The Drosophila SK channel (dSK) contributes to photoreceptor performance by mediating sensitivity control at the first visual network. J. Neurosci. *31*, 13897–13910. https://doi.org/10.1523/JNEUROSCI.3134-11.2011.

Please cite this article in press as: Chen et al., Sleep facilitates pattern separation through SK channel-mediated sparse coding, Current Biology (2026), https://doi.org/10.1016/j.cub.2026.02.028

STAR★METHODS

KEY RESOURCES TABLE

REAGENT or RESOURCE	SOURCE	IDENTIFIER
Antibodies		
Mouse monoclonal anti-Bruchpilot (1:50)	Developmental Studies Hybridoma Bank	RRID: AB_2314866
Goat anti-mouse Alexa Fluor 488 (1:400)	ThermoFisher	Cat# A-11001; RRID: AB_2534069
Goat anti-mouse Alexa Fluor 647 (1:400)	ThermoFisher	Cat# A-21235; RRID: AB_2535804
Chemicals, peptides, and recombinant proteins		
Mineral oil	Merck	330760
4-methyl-cyclohexanol	Merck	153095
3-octanol	Merck	218405
Pentyl acetate	Merck	109584
Acetic acid	Honeywell	A6283
AlexaFluor488-conjugated streptavidin (1:400)	ThermoFisher	S32357
AlexaFluor647-conjugated streptavidin (1:400)	ThermoFisher	S32354
PBS 10x	gibco	12579099
Paraformaldehyde	ThermoFisher	047377.9L
Triton X-100	Merck	T8787
Normal Goat Serum	Jackson Immuno Research Labs	005-000-121
SlowFade Gold antifade reagent	ThermoFisher	S36937
NaCl	Fisher Scientific GmbH	S/3120/63
KCl	Merck	P5405
$NaHCO_3$	Merck	S5761
NaH_2PO_4	Merck	S5011
$CaCl_2$	Merck	21115
$MgCl_2$	Merck	M1028
Trehalose	Merck	T9531
Glucose	Merck	G8270
Sucrose	Merck	S0389
TES	Merck	T5691
HEPES	Merck	H4034
MgATP	Merck	A9187
Na_3GTP	Merck	G6129
EGTA	Merck	E4378
K-gluconate	Merck	G4500
Biocytin	Merck	B4261
DMSO	Merck	276855
NS8593	Merck	492031
Deposited data		
Raw and analyzed data	This study	Zenodo: https://doi.org/10.5281/zenodo.18644411
Experimental models: Organisms/strains		
D. melanogaster: w[1118	Bloomington Drosophila Stock Center	BDSC_5905
D. melanogaster: MB010B	Bloomington Drosophila Stock Center	BDSC_68293
D. melanogaster: nSyb-IVS-phiC31	Bloomington Drosophila Stock Center	BDSC_84152
D. melanogaster: UAS-IVS-GCaMP6f	Bloomington Drosophila Stock Center	BDSC_52869
D. melanogaster: UAS-CD4-tdTomato	Bloomington Drosophila Stock Center	BDSC_35837
D. melanogaster: UAS-SPARC2-S-mCD8::GFP	Bloomington Drosophila Stock Center	BDSC_84148

(*Continued on next page*)

Please cite this article in press as: Chen et al., Sleep facilitates pattern separation through SK channel-mediated sparse coding, Current Biology (2026), https://doi.org/10.1016/j.cub.2026.02.028

Continued

REAGENT or RESOURCE	SOURCE	IDENTIFIER
D. melanogaster: UAS-SPARC2-D-Syn21-CsChrimson::tdTomato-3.1	Bloomington Drosophila Stock Center	BDSC_84143
D. melanogaster: UAS-Dcr-2.D(X)	Bloomington Drosophila Stock Center	BDSC_24644
D. melanogaster: UAS-mCD8::GFP	Bloomington Drosophila Stock Center	BDSC_29715
D. melanogaster: UAS-SK RNAi	Vienna Drosophila Resource Center	VDRC:v103985
D. melanogaster: UAS-RNAi Ctrl	Vienna Drosophila Resource Center	VDRC:v60100
D. melanogaster: LexAop-IVS-GFP-p10 (VK00005)	A gift from Gerald M. Rubin	N/A
D. melanogaster: VT43924-Gal4.2 (attP2)	A gift from Andrew C Lin[36]	N/A
D. melanogaster: VT43924-LexA::GAD (attP2)	This study	N/A
Software and algorithms		
MESc v3.5	Femtonics	https://femtonics.eu/femtosmart-software/
Fiji	ImageJ	https://imagej.net/software/fiji/
pClamp 11.3	Molecular Devices	https://www.moleculardevices.com/
Prism	GraphPad	https://www.graphpad.com/
R 3.6.3	R project	https://www.r-project.org/
idocr	Github	https://github.com/shaliulab/idocr
Other		
CPE (co-polyester) material	UltiMaker	https://ultimaker.com/materials/s-series-cpe/
Borosilicate glass capillaries	World Precision Instruments	1B150F-4

EXPERIMENTAL MODEL AND STUDY PARTICIPANT DETAILS

Fly husbandry

All *Drosophila melanogaster* strains were raised on standard cornmeal agar food at 25°C under a 12:12 h light:dark cycle with 50%-60% relative humidity. All experiments were conducted using mated female *Drosophila melanogaster*. All flies were maintained at a dim blue light environment in incubators.

Fly strains

The following stocks obtained from the Bloomington Drosophila Stock Center were used: *MB010B* (BDSC_68293), *UAS-SPARC2-S-mCD8::GFP* (BDSC_84148), *nSyb-IVS-phiC31* (BDSC_84152), *UAS-IVS-GCaMP6f* (BDSC_52869), *UAS-CD4-tdTomato* (BDSC_35837), *UAS-SPARC2-D-Syn21-CsChrimson::tdTomato-3.1* (BDSC_84143), *UAS-Dcr-2.D(X)* (BDSC_24644), and *UAS-mCD8::GFP* (BDSC_29715). Stocks obtained from the Vienna *Drosophila* Resource Center for RNAi experiment were as follows: *UAS-SK RNAi*[54] (VDRC103985), KK library control lines (*UAS-RNAi Ctrl*, VDRC60100). *LexAop-IVS-GFP-p10* is a gift from Gerald M. Rubin. *VT43924-Gal4.2*[36] are previously generated. *VT43924-LexA::GAD* was created via LR Clonase reaction between pCR8/GW/TOPO-VT43924 and pBPnlsLexA::GADflUw.[55] The resulting construct was inserted in attP2 by the University of Cambridge Fly Facility Microinjection Service. All fly lines were outcrossed in the wild-type w^{1118} (BDSC_5905) background for at least 5 generations, except the lines using in the RNAi experiments. (see key resources table).

The genotypes of the flies used for each experiment are following. For behavior experiments in Figures 1 and S1: +*; nsyb-phiC31, R13F02-p65.AD/ UAS-SPARC2-S-mCD8::GFP; R52H09-GAL4.DBD*/+. For *in vivo* Ca^{2+} imaging experiments in Figure 2: +*; R13F02-p65.AD/ UAS-IVS-GCaMP6f, UAS-CD4-tdTomato; R52H09-GAL4.DBD*/+. For electrophysiology experiments for Kenyon cells in Figure 3: +*; nsyb-phiC31, R13F02-p65.AD/ UAS-SPARC2-D-Syn21-CsChrimson::tdTomato-3.1; R52H09-GAL4.DBD*/+. For electrophysiology experiments for APL neurons in Figures 4B–4G and S2B–S2E: +*; nsyb-phiC31, R13F02-p65.AD/ UAS-SPARC2-D-Syn21-CsChrimson::tdTomato-3.1; R52H09-GAL4.DBD/ VT43924-LexA::GAD, LexAop2-IVS-myr::GFP*. For electrophysiology (Figures 4H–4J and S2F–S2I) and behavior (Figure 5) experiments with knockdown SK in APL neurons: 1.*UAS-Dcr-2.D*/+*; UAS-mCD8::GFP/ UAS-dSK RNAi; VT43924-Gal4.2*/+ and *UAS-Dcr-2.D*/+*; UAS-mCD8::GFP/ P{attP,y[+],w[3']}(RNAi Ctrl); VT43924-Gal4.2*/+.

METHOD DETAILS

Sleep behavior and sleep deprivation

Flies aged 3-4 days old post-eclosion were loaded individually into the tubes containing sugar agar (2% agar with 5% sucrose) for at least one night to monitor or manipulate their sleep. Locomotion activity of individual flies was recorded using a video-based tracking

Please cite this article in press as: Chen et al., Sleep facilitates pattern separation through SK channel-mediated sparse coding, Current Biology (2026), https://doi.org/10.1016/j.cub.2026.02.028

device, ethoscope with an acquisition rate at 2 Hz,[56] and a sleep event was defined by the inactive state for 5 min. Mechanical rotation of individual tubes for 1.5 s was triggered by immobility of respective flies for consecutive 10 s to achieve sleep deprivation with a closed-loop system as previously used in the lab.[57] By examining the distribution of sleep duration prior to the conditioning task, we found that most flies slept more than 40% of the time during the 12-hour nighttime period (4.8 hours). Therefore, we established 4.8 hours as the threshold for inclusion. In the normal sleep (NS) group, only flies that slept more than 4.8 hours were kept. In the sleep deprivation (SD) group, only flies that slept less than 4.8 hours were considered successfully sleep-deprived. For both sleep and sleep-deprived conditions, experiments were acquired at ZT0-3 with or without sleep deprivation one night before. For the condition of sleep recovery, experiments were conducted at ZT3-6. Sleep analysis was performed with adaptations to the rethomics pipeline[58] in R.

Learning behavior of individual flies

Olfactory learning behavior of individual flies was conducted in a versatile custom-built apparatus consisting of 20 chambers with two air inlets at each side and two vents in the middle of individual chambers.[29] Chambers consisted of 3D-printed enclosures (CPE, Ultimaker) with two glass slides as floors and ceilings, where the dimension of a chamber (in mm) was 50 × 5 × 1.5 (l × w × h). Chambers equipped with transparent glass slides coated with ITO (indium tin oxide) were applied to deliver electric shocks during aversive conditioning, whereas chambers equipped with non-ITO transparent glass slides were used in post-conditioning preference tests to avoid contextual memory confounding the performance in olfactory discrimination tasks. ITO coating with a grid pattern on the glass slides was designed to insulate the positive and negative electrodes (a hundred ITO electrodes with a width of 0.5 mm spaced by 0.1 mm apart). ITO glasses were connected to a 75-V DC source through relay modules to control delivery of electrical shocks. Chambers were illuminated by 940 nm LEDs below and recorded by a top camera (Basler ace) equipped with a Computar M0814-MP2 lens at a frame rate of 5 Hz. Real-time activity of individual flies was imaged using computerized video-tracking. Filtered and humidified air was tuned by a main flow controller and was split into two streams (2 l/min for each) for either side. The stream of each side was independently controlled by solenoid valves to switch the flow between the vials containing mineral oil or diluted odors in mineral oil and further distributed evenly to 20 chambers at a flow rate of 0.1 l/min for each side. Odors were diluted in the mineral oil at the following concentration: 1:375 for MCH (4-methyl-cyclohexanol, CAS No. 589-91-3, Sigma-Aldrich), 1:500 for OCT (3-octanol, CAS No. 589-98-0, Sigma-Aldrich), 1:10000 for PA (pentyl acetate, CAS No. 628-63-7, Sigma-Aldrich). Odor blends were mixed via manipulating the proportion of the air flow through the vials in which two sub-streams flowed at the rate of 0.4 l/min and 1.6 l/min for MCH and OCT, or vice versa. Odors were vented from the middle of chambers to a collection bottle for absorption of excessive odor. Odors were introduced to the chambers for 2 min to access the preference before and 20 min after aversive conditioning; only flies with performance index (PI) ranging from -0.25 to 0.25 in the preference test before conditioning were included. For aversive conditioning, flies were exposed to CS^+ odor for 1 min paired with twelve electric shocks at 0.2 Hz. 14 mm in the middle of chambers was defined as a decision zone, and the incidences entering from decision zone toward either side during the delivery of odors were quantified to calculate the PI of individual flies by the following equation:

$$PI = \frac{(E_{CS+} - E_{CS-})}{(E_{CS+} + E_{CS-})}$$

Where E_{CS+} represents the number of entrances into zone with CS^+ odor and E_{CS-} represents the number of entrances into zone with CS^- odor or air.

In vivo Calcium imaging

Flies were briefly cold-anesthetized and secured to a custom imaging holder by threading a fine string beneath the neck to immobilize the head. Wings, eyes, and the dorsal thorax were fixed using UV-curable glue, and the proboscis and legs were immobilized to minimize motion artifacts and suppress dopaminergic modulation associated with voluntary leg movements. A small window of cuticle was removed to expose the brain, and overlying air sacs and fat bodies on the posterior surface were gently cleared. All surgical procedures were performed in external saline containing (in mM): 103 NaCl, 3 KCl, 1.5 $CaCl_2$, 4 $MgCl_2$, 26 $NaHCO_3$, 5 TES, 1 NaH_2PO_4, 10 trehalose, and 10 glucose (pH 7.3, bubbled with 95% O_2/5% CO_2, 275 mOsm). Following dissection, the fly was transferred to a recording stage under a two-photon microscope (FemtoSmart Dual, Femtonics) and continuously superfused with the same saline. GCaMP fluorescence was excited using a mode-locked femtosecond laser (Chameleon Ultra II, Coherent) tuned to 920 nm, and emission was detected with a GaAsP detector (Hamamatsu Photonics). For each fly, a single imaging plane was selected to include ~200 clearly identifiable Kenyon cells, and a 3-min rest period was allowed before image acquisition. Images were acquired at 5 Hz using a galvo scanner and a 20× water-immersion objective (XLUMPLFLN20XW, Olympus), with a pixel resolution of 0.47 × 0.47 μm. Image acquisition and microscope control were performed using MESc v3.5 (Femtonics), and image series were exported as TIFFs for further analysis.

Odor stimulation

Odors were diluted in MO (mineral oil, CAS No. 8042-47-5, Sigma-Aldrich) at the following concentrations: 1:37.5 for MCH (4-methyl-cyclohexanol, CAS No. 589-91-3, Sigma-Aldrich), 1:50 for OCT (3-octanol, CAS No. 589-98-0, Sigma-Aldrich), 1:1000 for AAC (acetic acid, CAS No. 64-19-7, Honeywell), 1:1000 for PA (pentyl acetate, CAS No. 628-63-7, Sigma-Aldrich). For two mixed odor blends,

Please cite this article in press as: Chen et al., Sleep facilitates pattern separation through SK channel-mediated sparse coding, Current Biology (2026), https://doi.org/10.1016/j.cub.2026.02.028

4M:1O and 4O:1M were 1:46.875 for MCH and 1:250 for OCT and 1: 187.5 for MCH with 1:62.5 for OCT, respectively. Filtered and humidified mainstream (1.8 l/min) air was mixed with a sub-stream (0.2 l/min) flowed through vials filled with 10ml mineral oil, and the sub-stream was directed to other vials containing diluted odorant in 10 ml mineral oil via a custom-built solenoid valve system while receiving a TTL pulse from the microscope. The air/odor streams were split into an exhausted stream and a flow-controlled stream to the delivery tube with a flow rate of 0.15 l/min, which shorten the delay time to 1s from odor vials to the end of delivery tube and minimize the onset and offset artifact when the solenoid valve switches. Every fly received two series of odor presentation trials in a pseudo-random sequence in which the same odor was not given consecutively. Among all olfactory stimuli, mineral oil was included as a blank stimulus, it was always presented first in every recording. Each odor was given twice to ensure PNs processed the olfactory stimuli faithfully,[59] so only the response to each odor in the second time was adopted for data analysis. Imaging was incessantly acquired for 420 s over 14 odor presentation trials in which every trial consists of a 250 ms odor pulse triggered 5 s after the trial onset and with an inter-stimulus interval for 30 s.

Electrophysiological recordings

Flies were anesthetized on ice shortly before decapitation. Brains were dissected in the same external saline used for the calcium imaging experiments (see above), and the glial sheath surrounding the brain was removed to visualize the recording site. The dissected brain was immobilized on the recording chamber using a custom-made platinum anchor. Cell somata were targeted for patching under a 20× water-immersion objective (XLUMPlanFL, Olympus) and visualized using IR-DIC on an upright BX51WI microscope (Olympus) with the Slicescope (scientifica). Before patching, the perineural sheath was further removed to expose a clean surface using a suction pipette (~1 MΩ) connected to the pipette holder. Patch pipettes were fabricated from borosilicate glass capillaries (1.5 mm o.d./ 0.84 mm i.d., 1B150F-4, World Precision Instruments) using a Sutter P-1000 puller (Sutter Instrument). For Kenyon cell recordings, the pipettes were fire-polished by a microforge (MF-830, Narishige) under a ~35 psi air pressure backfilled by a picospritzer (Harvard Apparatus) to achieve a final resistance of 11–14 MΩ.[60,61] For APL recordings, the pipettes were fire-polished without a backfilled pressure to achieve a typical resistance of 6–9 MΩ. Polished pipettes were filled with the internal solution containing (in mM): 140 potassium gluconate, 10 HEPES, 1 EGTA, 4 MgATP, 0.5 Na_3GTP, 1 KCl, 13 biocytin. Whole-cell recordings were made with a MultiClamp 700B amplifier (Molecular Devices) equipped with a CV-7B headstage, lowpass-filtered at 3 kHz, and sampled at 10 kHz using a Digidata 1550B digitizer controlled through pCLAMP 10 (Molecular Devices). Data were corrected for liquid junction potential (Neher, 1992), and data analysis was performed in Clampfit (Molecular devices). Putative Kenyon cells were selected based on the anatomical location without knowing the cell types during recording, and only recordings with recognizable morphology of Kenyon cells were included. Only one recording was tempted from one hemisphere for a clean post-hoc identification of Kenyon cell types. APL recordings were guided by visualization of green fluorescence protein under epifluorescence, and partial tissue covering on the APL soma were removed if necessary. Resting membrane potential was taken immediately after break-in without holding current and compensation for the pipette capacitance and series resistance. After that, all properties (Figures 3, 4, and S2) were recorded with the neutralization of pipette capacitance and bridge balance for series resistance in current clamp. Cells were held at around −60 ± 5 mV by injecting a hyperpolarizing current.

For Kenyon cell recordings, only cells with a resting membrane potential below −50 mV and exhibiting spiking responses to depolarizing current injections were further analyzed. A 600 ms current ramp, from –2 to +30 pA, starting at a membrane potential of –60 ± 5 mV was injected to estimate spike threshold and afterhyperpolarization (AHP). The spike onset was detected by finding maximum in the time derivative of membrane potential in the ramp trace in which each spike waveform should contain clear upward and downward deflections for the distinction of spikes from EPSPs, and the membrane potential corresponding to the first spike onset in the ramp was defined as the spike threshold. AHP was detected by the downward peak following the first spike and was estimated by the difference between spike threshold and downward peak. Input resistance, membrane time constant, and firing rate were estimated by a series of current steps consisting of a 500 ms hyperpolarizing current (–1 pA) followed by 750 ms current steps (1 pA increments, starting at −5 pA) 1 s apart from the constant hyperpolarizing step. Input resistance was calculated from the average change of steady-state voltage elicited by the constant hyperpolarizing current. Membrane time constant was determined by fitting a single exponential to the averaged voltage deflection responded to the constant hyperpolarizing current. Firing rate was the spike counts elicited by the 750ms current steps. After the recording, the brain was immediately fixed in 4% paraformaldehyde at room temperature for 20 min for further post-hoc staining.

For APL recordings, input resistance, membrane time constant, AHP were estimated by a series of current steps consisting of a 500 ms hyperpolarizing current (–50 pA) followed by 500 ms current steps (50 pA increments, starting at −100 pA) 1 s apart from the constant hyperpolarizing step. Bump responses and AHPs were elicited by high discharge in membrane potential, so the amplitudes were estimated by the deflection of membrane potential in response to 1 nA current injection during charging and after deactivation, respectively. To assess the channel contribution to the enhanced AHP in sleep-deprived flies, we estimated the decay time constant by exponential curve fitting. However, this method is not applicable in the normal sleep group, since many recordings exhibited low-amplitude AHPs, for which exponential fitting yielded unreliable decay estimates. Therefore, for cross-condition comparisons, AHP kinetics were quantified as the time required for the membrane potential to decay from 70% to 30% of the peak AHP amplitude. For pharmacological experiments, NS8593 (492031, Sigma-Aldrich), rather than another selective inhibitor - apamin, was applied to block *Drosophila* SK channels, since fly SK has been reported insensitive to apamin.[62] 10 mM stock of NS8593 in dimethyl sulfoxide (DMSO, CAS No. 67-68-5, Sigma-Aldrich) was dissolved in the external saline, yielding NS8593 at a final concentration of 10 uM with

Please cite this article in press as: Chen et al., Sleep facilitates pattern separation through SK channel-mediated sparse coding, Current Biology (2026), https://doi.org/10.1016/j.cub.2026.02.028

0.1 % DMSO (v/v). 0.1% DMSO (v/v) was added in the external saline as vehicle control, and the difference on AHP amplitude in response to 1 nA current was calculated by the responses before and 20 min after treatment of NS8593.

Sample sizes varied across intrinsic excitability parameters because not all parameters could be obtained from every recorded cell, and some features could not be detected by Clampfit in all recordings. All available measurements were included for each parameter whenever possible.

Immunofluorescence and confocal imaging

Fly brains acquired after electrophysiology experiments were washed in PBS with 0.5% Triton X-100 (PBST) for 15 min each time. After washing for three times in PBST, brains were incubated in PBST containing 5% normal goat serum for 25 min at room temperature, and then incubated with mouse nc82 (Development Studies Hybridoma Bank, 1:50) overnight at 4 °C. Subsequently, brains were incubated with secondary antibodies including Alexa 488 or Alexa 647 anti-mouse (Invitrogen, 1:400) and Alexa 488- or Alexa 647-conjugated streptavidin (Invitrogen, 1:400) for 2 hours at room temperature. Brains were washed in PBST three times for 15min at room temperature after every incubation step with antibodies or Alexa Fluor Dyes. After the final washing step, brains were mounted in Vectashield (Vector Labs), and images were acquired using Nikon NiE A1R confocal microscopy with a 1μm step-size under 40x magnification.

QUANTIFICATION AND STATISTICAL ANALYSIS

Image processing and analysis

Fluorescence image stacks were processed and analyzed using ImageJ/Fiji software. Motion correction was first applied to all imaging sessions using the Fiji plugin TurboReg to correct the drift in the x-y plane. Recording with significant z-drift, uncorrectable motion artifacts, or obvious structure distortion were excluded from further analysis. After image registration, regions of interest (ROIs) corresponding to individual Kenyon cell somata in the mushroom body were manually identified from the motion-corrected average intensity projection image across all frames. Using ImageJ's ROI Manager, circular ROIs (typically 3–5 μm in diameter) were drawn around clearly distinguishable somatic boundaries based on baseline fluorescence morphology. Only ROIs with consistent shape, size, and signal quality across trials were retained. Approximately 150–200 Kenyon cells were selected per preparation depending on visibility. For each ROI, fluorescence intensity was extracted over time and used to calculate the fractional change in fluorescence ($\Delta F/F_0$). Baseline fluorescence (F_0) was defined as the mean fluorescence during the 6-s window preceding odor delivery. Response fluorescence (F_t) was calculated as the mean fluorescence during a 6-s window following odor onset. The response window was chosen to capture the full calcium transient evoked by the brief (250 ms) odor pulse, which persisted for several seconds. Within each trial, ΔF was calculated as the difference between response and baseline fluorescence, and $\Delta F/F_0$ was computed as:

$$\Delta F / F_0 = (F_t - F_0) / F_0$$

Population sparseness

To access the sparseness of odor representations in the mushroom body, olfactory responses to each stimulus across multiple trials were computed for each ROI. Response of an ROI was considered significant if the odor-evoked response ($\Delta F/F_0$) exceeded baseline by 3 s.d. (σ); otherwise, the ROI was classified as unresponsive. (A 3σ threshold corresponds to the top ~0.3% of a normal distribution.) Population sparseness (S_p) was calculated for each odor across all ROIs (e.g., Kenyon cells) using the following equation[20]:

$$S_p = \frac{1}{1 - \frac{1}{N}} \left(1 - \frac{\left(\sum_{i=1}^{N} \frac{r_i}{N} \right)^2}{\sum_{i=1}^{N} \frac{r_i^2}{N}} \right)$$

Where r_i is the normalized response ($\Delta F/F_0$) of ROIi to the odor and N is the total number of ROIs.

Inter-Odor correlation

To assess the similarity of population representations across odors, we computed the Pearson correlation coefficient (r) between the response vectors (across all ROIs) for each pair of odors. For a given pair of odors A and B:

$$r_{AB} = \frac{\sum_{i=1}^{n} (A_i - \overline{A})(B_i - \overline{B})}{\sqrt{\sum_{i=1}^{n} (A_i - \overline{A})^2 \sum_{i=1}^{n} (B_i - \overline{B})^2}}$$

Where A_i and B_i are responses of ROI_i to odors A and B, respectively. Correlation matrices were visualized to compare representational overlaps across the odor panel. For a given odor pair, Pearson correlation coefficients for each fly were Fisher r-to-z

Please cite this article in press as: Chen et al., Sleep facilitates pattern separation through SK channel-mediated sparse coding, Current Biology (2026), https://doi.org/10.1016/j.cub.2026.02.028

transformed, and differences across sleep conditions were assessed using ordinary one-way ANOVA followed by Tukey's multiple comparisons test.

Statistical analyses

Data were analyzed using Prism 10 (GraphPad). For comparisons of two matched groups, paired t-test or Wilcoxon's matched pairs test were applied for normally or non-normally distributed data, respectively. For comparison of unpaired groups, unpaired t-test or Mann-Whitney U-tests. Current versus firing rate relationships were analyzed using Repeated measures two-way ANOVA, followed by Bonferoni post-hoc tests.